Electronic Supplementary Material (ESI) for Nanoscale Advances.
This journal is © The Royal Society of Chemistry 2023

Supporting Information

Absolute Energy Levels in Nanodiamonds of Different Origins and Surface Chemistries

Daria Miliaieva,*[a,e] Aurelien Sokeng Djoumessi,[b,c] Jan Cermak,[a] Katerina Kolarova,[a] Maximilian Schaal,[d] Felix Otto,[d] Ekaterina Shagieva,[a] Olexandr Romanyuk,[a] Jiri Pangrac,[a] Jaroslav Kulicek,[e] Vojtech Nádaždy,[f,g] Stepan Stehlik[a,h] Alexander Kromka,[a] Harald Hoppe [b,c] Bohuslav Rezek[e]

[a]*Institute of Physics, Czech Academy of Sciences, Na Slovance 1999/2, 182 21 Prague 8, Czech Republic*

[b]*Center for Energy and Environmental Chemistry Jena (CEEC Jena), Friedrich Schiller University Jena, Philosophenweg 7a, 07743 Jena, Germany*

[c]*Laboratory of Organic and Macromolecular Chemistry (IOMC), Friedrich Schiller University Jena, Humboldstrasse 10, 07743 Jena, Germany*

[d]*Institute of Solid State Physics, Friedrich Schiller University Jena, Helmholtzweg 5, 07743 Jena, Germany*

[e]*Faculty of Electrical Engineering, Czech Technical University in Prague, 166 27 Prague, Czech Republic*

[f]*Institute of Physics, Slovak Academy of Sciences, Dúbravská cesta 9, 845 11 Bratislava, Slovak RepublicRepublic*

[g]*Centre for Advanced Material Application, Slovak Academy of Sciences, Dúbravská cesta 9, 845 11 Bratislava, Slovak Republic*

[h]*New Technologies – Research Centre, University of West Bohemia, Univerzitní 8, 306 14, Pilsen, Czech Republic*

Energy-Resolved Electrochemical Impedance Spectroscopy (ER-EIS)

ER-EIS is a novel technique originally used to map the electronic density of states (DOS) in organic semiconductors [V. Nadazdy, F. Schauer, K. Gmucova, Appl. Phys. Lett. 2014, 105, 142109]. This method measures the impedance of the semiconductor film/electrolyte system at a frequency, where the redox reaction dominates and other electrochemical processes are eliminated. The redox reaction then determines the charge-transfer resistance, R_{ct}, which is evaluated from the real part of the impedance. The DOS function g(E) can be then determined directly from the obtained $R_{ct}(E_F)$ function, where the Fermi energy $E_F = eU$ is given by the applied voltage U:

$$g(E_F) = \frac{1}{e^2 k_{et}[A] S R_{ct}(E_F)} ,$$

where e is the elemental charge, k_{et} is the charge-transfer coefficient (~10^{24} cm^{4}s^{-1}), [A] is the concentration of the redox species dissolved in the solvent (6x10^{19} cm^{-3}), and S is the area of the working electrode [F. Schauer, V. Nadazdy, K. Gmucova, J. Appl. Phys. 2018, 123, 161590]. By sweeping the applied voltage U it is possible to map the DOS in a wide energy range.

Experimentally, ER-EIS measurements were performed in electrochemical microcells with a volume of about ≈200 µL, which were formed by glueing the set of plastic cones on nanodiamond layers spin-coated on the ITO substrate. A three-electrode configuration was used, with the nanodiamond layer as the working electrode, Ag/AgCl as the reference electrode and a platinum wire as the auxiliary electrode. The applied bias voltage adjusted relative to the Ag/AgCl electrode was recalculated to the energy scale, assuming the Ag/AgCl energy vs. vacuum value of − 4.66 eV. The active working electrode area S was 12 mm^2. The solution of 0.1 m

$TBAPF_6$ in anhydrous acetonitrile was used as the supporting electrolyte. To avoid intercalation of ions the measurement of the whole spectrum is performed in two steps, always in a new electrochemical cell, with one measurement being used to obtain the branch for the hole-transporting states and one for the electron-transporting states. [V. Nadazdy, F. Schauer, K. Gmucova, Appl. Phys. Lett. 2014, 105, 142109; H. Bässler, D. Kroh, F. Schauer, V. Nádaždy, A. Köhler, Adv. Funct. Mater. 31 (2021) 2007738]. The impedance/gain-phase analyzer (Model 1260, Solartron Analytical, UK) was employed in connection with a homemade potentiostat in the standard three-electrode configuration. The AC signal frequency and the RMS value of AC voltage were set to 0.5 Hz and 100 mV, respectively. The measurements were performed in a glove box with a protective N_2 atmosphere (oxygen and moisture below 20 ppm and 2 ppm, respectively).

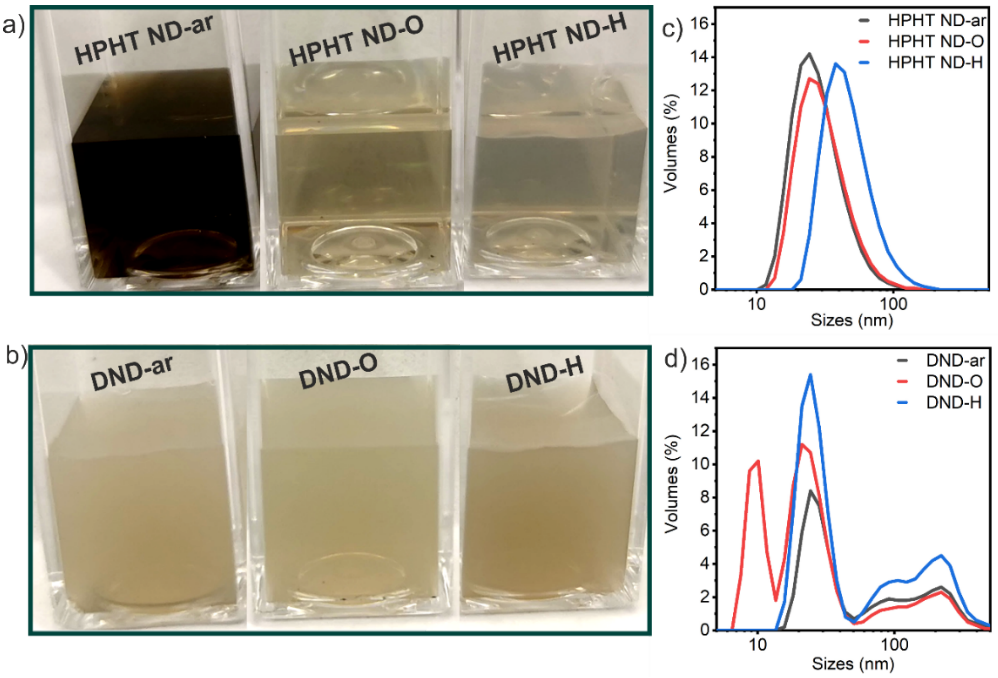

Figure S1. Photo of aqueous colloidal solutions (1mg/ml) of HPHT (a) and DND (b). Particle size distribution in water established by DLS (c, d) shows the dominant size of the particles is similar independently of the origin and thermal annealing does not change the size distributions significantly. Noteworthy, besides the dominant size fraction of aggregated primary particles (with the maximum at ~20 nm) DNDs contain micrometre-sized aggregates. DND-O contain a sub-10 nm fraction upon air annealing due to partial annealing of the main fraction. HPHT NDs show a similar size distribution curve (with the maximum at ~20 nm), however, (i) the peak is broader and (ii) hydrogenation of HPHT upshifts the mean size due to the hydrophobicity of the particles and their aggregation in water.

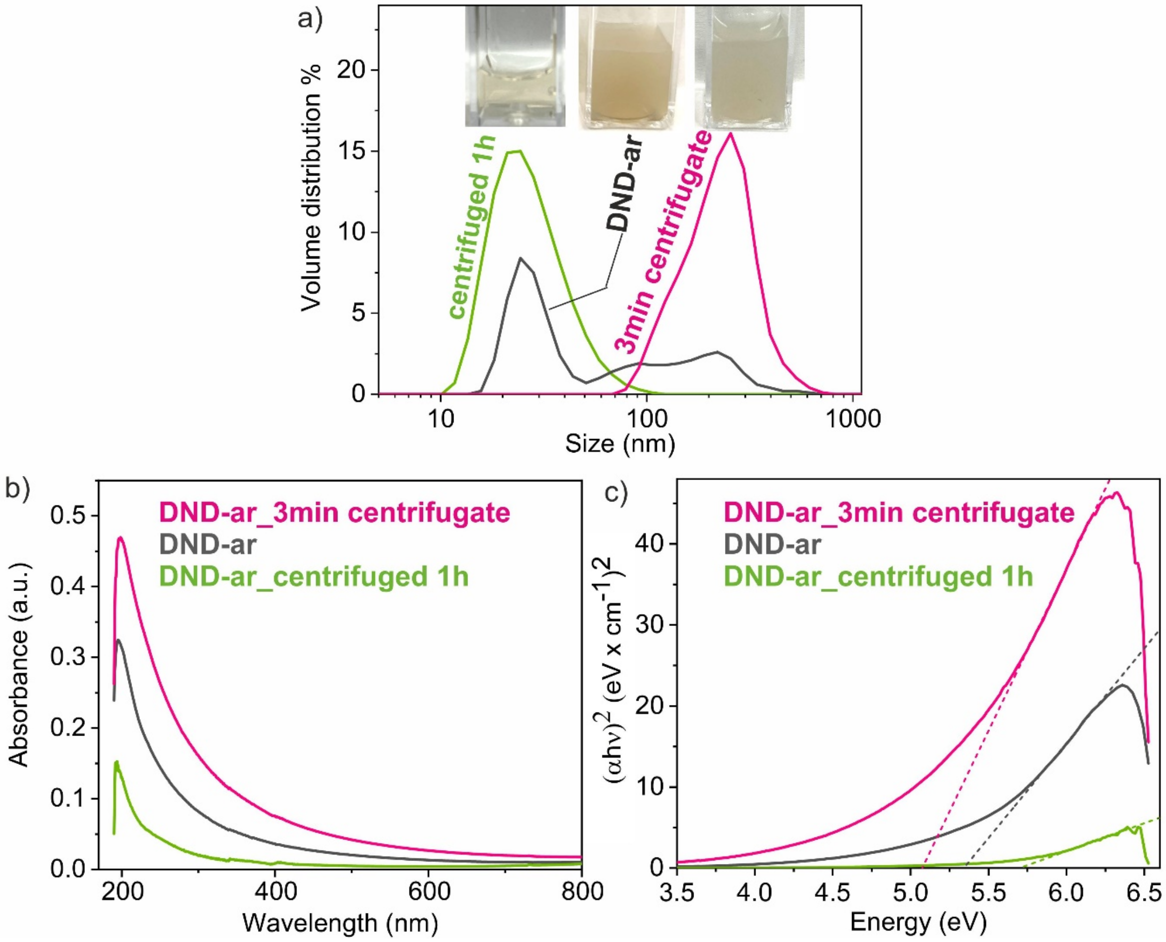

Figure S2. a) DND-ar fractionation confirmed by DLS b) UV-VIS absorbance of DND-ar fractions c) Tauc plots of DND-ar fractions with tangents for energy band gap (E_g) determination. This experiment demonstrates that a DND-ar fraction of 70 - 700 nm causes pronounced scattering, which contributes to the apparent E_g = 5.1 eV. This fraction results in turbidity of the DNDs colloids as can be seen from the inset photos.

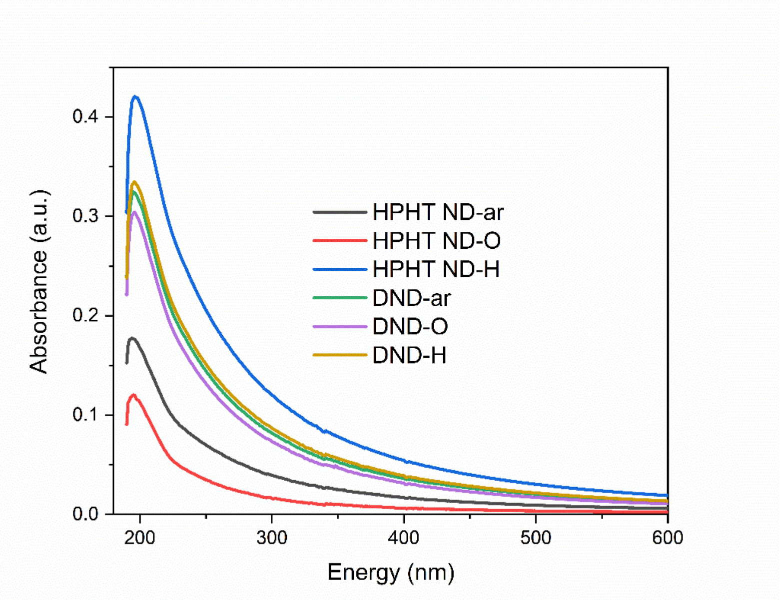

Figure S3. ND absorbance spectra.

Figure S4 shows the spectra of the C 1s core levels for a) HPHT, b) DND, and c) the normalized spectra from the Au substrates. Spectra positions were calibrated with respect to the position of the Au 4f$^{7/2}$ peak maxima at 84 eV. The C 1s peak position of the adventitious carbon on the Au reference substrate (adv. C/Au) lies at 285 eV. The positions of the C 1s peaks of the ND samples depend on the electronic properties of materials and evident that photoemitted electrons in HPHT ND-H have ~ 1.6 eV less core level electrons binding energy than in DNDs and oxidised HPHTs.

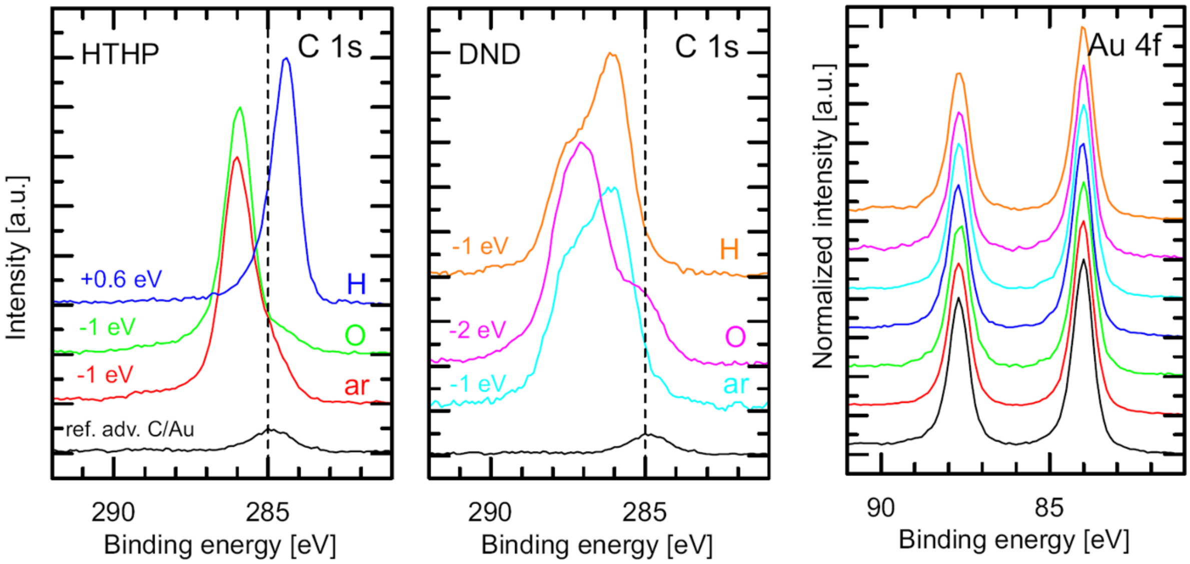

Figure S4. C 1s spectra measured on a) HPHT and b) DND differently terminated samples. c) Au 4f spectra from reference Au substrate and from overlayer of NDs on Au. Shifts of C 1s positions are related to the different core C 1s binding energy of electrons.

Table S1 shows values of the full width at half maximum (FWHM) of sp^3 C 1s peaks obtained by XPS. The FWHM of the HPHT ND samples (0.8 - 1.1 eV) is more than twice as narrower compared to the FWHM of the DND samples (2.0 - 2.5 eV). It corroborates the more defective nature of DNDs compared to HPHTs revealed by Raman spectroscopy.

Table S1.

The full width at half maximum (FWHM) of C 1s XPS peak in NDs.

	FWHM, eV (sp^3)		FWHM, eV (sp^3)
HPHT ND-ar	1.1	DND-ar	2.5
HPHT ND-O	0.9	DND-O	2.0
HPHT ND-H	0.8	DND-H	2.5

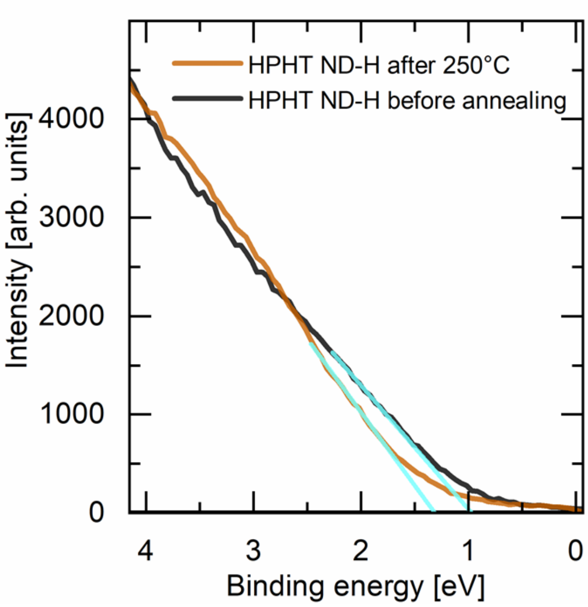

Figure S5. Determination of the UPS binding energy cut-off of HPHT ND-H before and after heating at 250 ^{0}C for 1h. The cut-off indicates the VBM position is 0.3 eV upshifted relative to Fermi level (at 0 eV binding energy) in ambient conditions compared to the HPHT ND-H surface without adsorbates due to band bending.